THERMAL PERFORMANCE AND CAPILLARY LIMIT OF A CERAMIC CAPILLARY EVAPORATOR USED IN LHP AND CPL

Paulo Henrique Dias dos Santos, paulosantos@labcet.ufsc.br
Edson Bazzo, ebazzo@emc.ufsc.br
Federal University of Santa Catarina, Department of Mechanical Engineering, LabCET - Laboratory of Combustion and Thermal Systems Engineering - Campus Universitário, 88.040-900, Florianópolis, SC, Brazil

Abstract. *In this paper the thermal performance and experimental results of a ceramic wick working as capillary evaporator of Loop Heat Pipe (LHP) and Capillary Pumped Loop (CPL) are presented. One LHP and one CPL were manufactured with the similar capillary evaporators with ceramic wick. The LHP has a capillary evaporator with* 10 *mm of inner diameter and* 25 *mm of length, its compensation chamber has the same diameter as the evaporator and length of* 50 *mm, its transport lines of liquid and vapor have* 2.8 *mm of inner diameter and its condenser has* 120 *mm of length. The CPL has a capillary evaporator with* 10 *mm of inner diameter and* 50 *mm of length (*25 *mm of evaporation area), its transport lines of liquid and vapor have* 2.8 *mm of inner diameter and its condenser has* 385 *mm of length. The ceramic wick applied to LHP and CPL has* 50% *of porosity,* 1 *to* 3 μ*m pore size distribution and permeability of about* 35×10^{-15} m^2*. The performance tests were carried out for the LHP and CPL using deionized water as working fluid for power inputs up to* 30 *W. The thermal performance, the capillary limit and the total thermal resistance of these systems are also presented.*

Keywords: *LHP, CPL, Ceramic Wick, Water*

1. Introduction

In the last years it has been studied the reliability and applicability of the LHPs and CPLs regarding the thermal control of electronic equipments. This study consist of an analysis of the thermal behavior of LHPs and CPLs taking into account changes in the working fluid, number of evaporators and condenser, inclination of the systems, materials for the systems and materials for the porous wicks (Reimbrecht, 2004; Berti, 2008 and Santos et. al., 2010).

The porous wick characteristics, such as the effective thermal conductivity, the pore diameter, the porosity and the permeability, have a significant effect on the CPL and LHP Performance. Nowadays, most LHPs and CPls use polyethylene or metallic wicks in the evaporator. There is no any CPL using ceramic wick and only few LHPs using it (Rassamakin et. al., 2002; Rhi, 2006 and Santos et. al., 2010).

This work continues the work published by Santos et. al. (2010). However, here it is presented a theoretical and experimental analysis of the ceramic wick applicability and reliability in one LHP and one CPL. The application of this ceramic wick is an alternative to wicks made of metal and plastic. The thermal performance, the capillary limit and the total thermal resistance of these systems are presented. The performance tests were carried out for power inputs ranging from 5 to 15 W for the LHP and from 5 to 30 W for the CPL.

2. Experiment

In this work one LHP and one CPL were manufactured and tested in order to evaluate their thermal performance and their applicability in thermal control of microprocessors and electronic components in general. The surface temperatures at the main part of the systems, e.g. evaporator and condenser inlet and outlet, compensation chamber (in case of LHP) and reservoir (in case of CPL) were measured while the thermal load was varied. Both systems used water as working fluid. The systems used a ceramic wick in the capillary evaporator. For the heating of the capillary evaporators, electric resistors (cartridge heaters inside of copper block for the LPHs and heaters in format of wire for the CPL) were used to simulate the heat generation in microprocessors and electronic components. The condenser of the LHP was cooled using water in forced convection and the condenser of CPL was cooled using air also in forced convection.

Figure 1(a) shows the LHP and its capillary evaporator has 10 mm of inner diameter and 25 mm of length, the compensation chamber has the same diameter of the evaporator and length of 50 mm, the transport lines of liquid and vapor have 2.8 mm of inner diameter and the condenser has 120 mm of length. Figure 1(b) shows the CPL and its capillary evaporator has 10 mm of inner diameter and 50 mm of length (25 mm of evaporation area), transport lines of liquid and vapor have 2.8 mm of inner diameter and the condenser has 385 mm of length.

The ceramic wick applied to LHP and CPL has 50% of porosity, 1 to 3 μm pore size distribution and permeability of about 35×10^{-15} m^2. Figure 2(a) depicts a view of the evaporator, the compensation chamber and the ceramic wick of the LHP. Only the upper side of the capillary evaporator has grooves and four grooves were machined in the ceramic wick used for the LHP. Along the work the machining technique was improved and it was possible to machine more vapor channels (12 grooves) in the ceramic wick used for the CPL, Fig. 2(b). A thermal cleaning at 800^oC for 60 min is applied to remove the oil contamination after the machining. Figure 2(b) presents a view of the evaporator and the ceramic wick

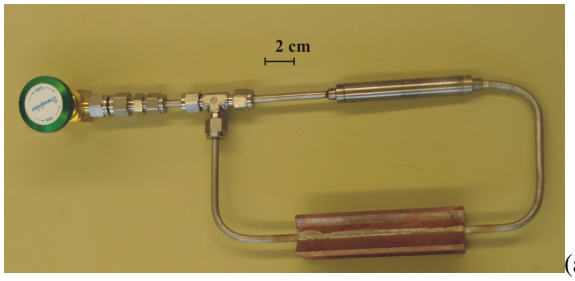

(a)

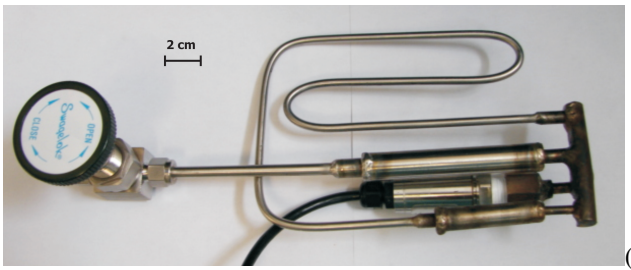

(b)

Figure 1. (a) General view of the LHP (b) CPL.

of the CPL. Contrary to the wick for the LHP, all the circumference of capillary evaporator for the CPL has grooves.

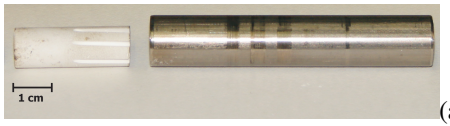

(a)

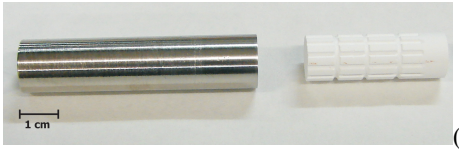

(b)

Figure 2. (a) Ceramic wick with vapor channels (grooves) used in the LHP (b) CPL.

The temperature distribution along the LHP was measured using thermal resistors (Pt100). Figure 3(a) depicts the locations of the temperature sensors: evaporator outlet ($T_{Evap,out}$), condenser inlet ($T_{Cond,in}$), condenser outlet ($T_{Cond,out}$), evaporator inlet ($T_{Evap,in}$) and the compensation chamber (T_{CC}). The temperature distribution along the CPL was measured using temperature sensors (thermocouples type T). Figure 3(b) depicts the locations of the temperature sensors: evaporator (T_{Evap}), evaporator outlet ($T_{Evap,out}$), vapor line ($T_{VaporLine}$), condenser inlet ($T_{Cond,in}$), condenser (T_{Cond}), condenser outlet ($T_{Cond,out}$), evaporator inlet ($T_{Evap,in}$), reservoir (T_{Res}) and reservoir outlet ($T_{Res,out}$).

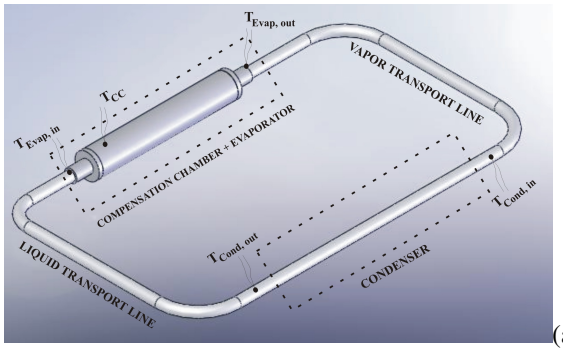

(a)

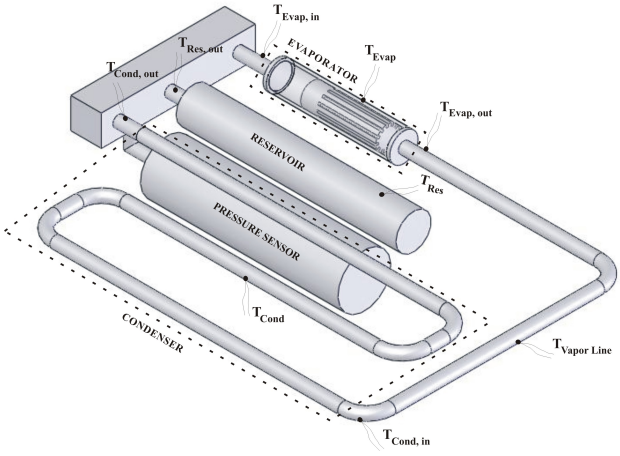

(b)

Figure 3. (a) Positions of the thermal sensors along the LHP (b) CPL.

The LHP and CPL were first adjusted to the horizontal position and the ambient temperature was set. Once all temperatures of the LHP or CPL showed the same value as the ambient temperature ($\Delta T_{max} = 1^o$ C), the first power input step of 5 W was applied to the evaporator. Once all temperatures reached a stationary value (or oscillating stationary value), the power input was increased by steps of 5 W. The electrical power (P_{el}) applied to the cartridge was calculated by measuring the current and the voltage accross it. Assuming no heat losses through the insulation at the heating zone, the applied electrical power is taken as the heat applied to the systems. The performance tests were carried out for power inputs ranging from 5 to 15 W for the LHP and from 5 to 30 W for the CPL.

For LHP, including the accuracy of the temperature sensors and the uncertainties of the data logger, the uncertainty of the temperature is estimated at ± 0.5 K. The uncertainty of the electrical power input is estimated at $\pm 0.5 \times 10^{-3}$ W including the uncertainty of the power supply unit and the uncertainty of the data logger. The temperature sensors (RTDs) are of type Pt100 delivered with an accuracy of class A. Regarding to international norm IEC 751, for a maximum temperature of 100 ^{o}C, the uncertainty of the sensor is $u_{Pt100} = \pm 0.35\ K$. For the CPL, the uncertainty of the measurements were estimated for the temperature and power input. Taking into account the accuracy of the temperature sensors (thermocouples type T) and the uncertainties of the data logger (Agilent 34970A with 20 channels), the uncertainty of the temperature measured was evaluated to be ± 1 ^{o}C. The uncertainty of the electrical power input is evaluated to be ± 0.06

W including the uncertainty of the power supply unit and the uncertainty of the data logger (Agilent N6700B).

3. Capillary Limit Analysis of the LHP and the CPL

The main operational limits of capillary pumping systems (CPL and LHP) are the boiling and capillary limits. Here, only the capillary limit will be studied. The condition for both CPL and LHP work is that the total system pressure drop does not exceed the maximum pressure that the porous wick can provide. Due to the vapor penetration through the porous wick, the operating temperature of the system has a sudden increase when the capillary limit is exceeded. So, the capillary pumping system operation requires that the sum of the pressure drops in the components and in the transport lines must be smaller than the maximum capillary pressure head developed by the wick, i.e.,

$$\Delta P_{cap,\max} = \frac{2\sigma}{r_p} \geq \Delta P_{\text{evap}} + \Delta P_{\text{cond}} + \Delta P_{\text{v}} + \Delta P_{\text{l}} + \Delta P_{\text{g}} \tag{1}$$

In Eq. 1 the pressure losses are identified as: ΔP_{evap} - pressure losses in the evaporator, ΔP_{cond} - pressure losses in the condenser, ΔP_{v} - pressure losses in the vapor lines, ΔP_{l} - pressure losses in the liquid lines and ΔP_{g} - pressure losses due to the gravity action.

In the following, the total pressure drop will be estimated and compared to the expected maximum capillary limit.

3.1 Mass Flow Rate

The mass flow rate can be approximately obtained by the energy balance in the compensation chamber and capillary evaporator assembly during steady-state operation. During typical LHP operation, heat is applied uniformly to the evaporator (Q_{app}). The majority of the overall applied heat load (Q_{evap}) vaporizes the liquid on the outer surface of the porous wick and superheats the vapor in the vapor channel up to the outlet of the evaporator. The other part of the applied heat load is transferred through the metallic structure of the assembly to the compensation chamber, where one part is transferred to the ambient by natural convection $Q_{cc,amb}$, and the other part is transferred to the vapor transport line. Here the heat transfer to the vapor transport line will be neglected. So, the energy balance in the compensation chamber and evaporator is:

$$Q_{app} = Q_{evap} + Q_{cc,amb} \tag{2}$$

where

$$Q_{evap} = \dot{m}\ h_{lv} + \dot{m}\ c_{p,l}\ (T_{evap,out} - T_{evap,sat}) + \dot{m}\ c_{p,l}\Delta T_{subcooled} \tag{3}$$

For heat transfer from the compensation chamber surface to the ambient, the heat transfer coefficient from the outer wall to the ambient is assumed to be that of natural convection. The outer heat transfer coefficient $h_{cc,amb}$ of a horizontal cylinder to the ambient can be estimated by (Holman, 1990),

$$h_{cc,amb} = 1.32 \left(\frac{T_{cc}^{w} - T_{amb}}{d_{cc,out}} \right)^{0.25} \tag{4}$$

Where $d_{cc,out}$ is the outer diameter of the compensation chanber, T_{cc}^{w} is the temperature measured at the wall of the compensation chamber, T_{amb} is the ambient temperature.

The effects of the sensible heat in the mass flow rate are only secondary in most cases and can be neglected ($\dot{m}\ h_{lv} \gg \left[\dot{m}\ c_{p,l}\ (T_{evap,out} - T_{evap,sat}) + \dot{m}\ c_{p,l}\Delta T_{subcooled}\right]$). From the applied heat (Q_{app}), the mass flow rate can be estimated from,

$$Q_{app} = \dot{m}\ h_{lv} + h_{cc,amb}A_{cc,out}(T_{cc}^{w} - T_{amb}) \tag{5}$$

Since the reservoir in CPL is separated from the evaporator and assuming that there is no heat transfer from the evaporator to the ambient (due to insulation of the evaporator), so the mass flow rate can be obtained as $Q_{app} = \dot{m}\ h_{lv}$.

3.2 Fluid Properties

The fluid properties used in this work were obtained from the software Engineering Equation Solver (EES). These properties include saturation pressure, latent heat, liquid and vapor densities, liquid and vapor viscosities, liquid and vapor thermal conductivities, liquid and vapor specific heats and liquid surface tension.

3.3 Single-Phase Pressure Drop

It is assumed single-phase flow along the grooves, vapor and liquid transport lines, liquid feeding channel and through the porous wick. The single-phase viscous pressure drop can be estimated from the Darcy-Weisbach equation,

$$\Delta p = f\left(\frac{L}{d_h}\right)\left(\frac{\rho v^2}{2}\right). \tag{6}$$

Where f is the Darcy (or Moody) friction factor. For laminar flow in circular tubes, $f = 64\mathrm{Re}^{-1}$. For turbulent flow in smooth tubes, the solution proposed by H. Blasius, $f = 0.316\mathrm{Re}^{-0.25}$ for $4000 < Re < 10^5$, is used.

In the vapor grooves (dimensions $h_{groove} \times w_{groove}$), the hydraulic (equivalent) diameter is,

$$d_h = \frac{2h_{grovve}w_{groove}}{(h_{grovve} + w_{groove})} \tag{7}$$

For the vapor and liquid transport lines the hydraulic (equivalent) diameter is the inner diameter (d_{in}).

The pressure drop in the porous wick, according to Darcy's law, can be can calculated as,

$$\Delta p_w = \frac{\dot{m}_l \mu_l}{\theta \rho_l 2\pi L_w k_w} \ln\left(\frac{r_{w,out}}{r_{w,in}}\right). \tag{8}$$

Where $\theta = \dfrac{N_{groove}w_{groove}}{2\pi r_{w,out}}$ is the is the comprehended angle by the grooves, N_{groove} is the number of grooves in the wick.

3.4 Condenser

In general, the condenser presents superheated vapor, two-phase and subcooled liquid regions. Single phase equations as before are used for the superheated vapor and subcooled liquid regions. For the two-phase region, first its lenght must be determined. For that it is necessary to apply an energy balance in the condenser as shown in Fig. 4.

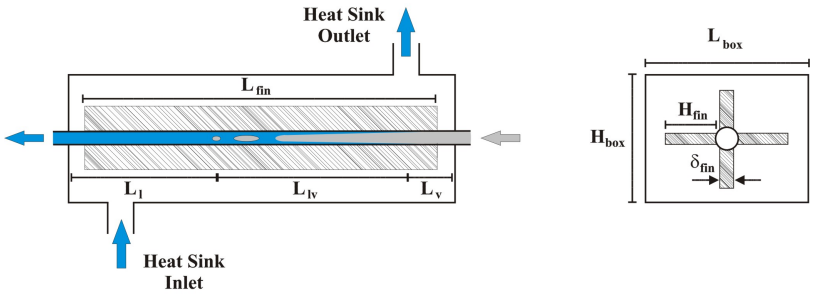

Figure 4. Schematic diagram of the condenser with finned tube.

In Fig. 4 $L_{cond,v}$ is vapor length in the condenser, $L_{cond,lv}$ is two phase length in the condenser and $L_{cond,l}$ is liquid length in the condenser.

The energy balance in the superheated vapor region provides:

$$\dot{m}\, c_{p,v}\left(T_{cond,in} - T_{cond,sat}\right) = (UA)_{cond,v}\, \Delta T_{lm}^{cond,v} \tag{9}$$

where,

$$\Delta T_{lm}^{cond,v} = \frac{\Delta T_1^{cond,v} - \Delta T_2^{cond,v}}{\ln\left(\Delta T_1^{cond,v} \Big/ \Delta T_2^{cond,v}\right)}$$

$$\Delta T_1^{cond,v} = T_{cond,in} - T_{HS,out} \tag{10}$$

$$\Delta T_2^{cond,v} = T_{cond,sat} - T_{HS,in} \tag{11}$$

$$(UA)_{cond,v} = \frac{1}{\dfrac{1}{h_{cond,v}\left(\pi d_{cond,in} L_{cond,v}\right)} + \dfrac{\ln\left(d_{cond,out}/d_{cond,in}\right)}{2\pi\lambda_{SS} L_{cond,v}} + \dfrac{1}{\eta_{fin,0} h_{HS} A_t}}. \tag{12}$$

A finned tube is used in the condenser section and the overall surface efficiency of the fin ($\eta_{fin,0}$) may be determined from

$$\eta_{fin,0} = 1 - \left(1 - \eta_{fin}\frac{A_{fin}}{A_u}\right) \tag{13}$$

where the finned (A_{fin}), unfinned (A_u) and total(A_t) areas and the fin efficiency (η_{fin}) are defined as,

$$A_{fin} = N_{fin}L_{fin}\left(2H_{fin} + \delta_{fin}\right) \tag{14}$$

$$A_u = \pi d_{cond,out}L_{fin} - N_{fin}L_{fin}\delta_{fin} \tag{15}$$

$$A_t = A_u + A_{fin} \tag{16}$$

$$\eta_{fin} = \frac{\tanh\left(mH_{fin}\right)}{mH_{fin}}, \text{ where } m = \sqrt{\frac{2h_{HS}}{\delta_{fin}\lambda_{fin}}}; \eta_{fin} \ll H_{fin}. \tag{17}$$

The heat transfer coefficient of the water flow in the heat sink (h_{HS}) is estimated from

$$h_{HS} = \frac{Nu_{HS}\lambda_{water}}{d_e} \tag{18}$$

where the equivalent diameter (d_e) based on the heat transfer area is defined as,

$$d_e = \frac{4A_c}{P_h} \tag{19}$$

where the heat transfer perimeter (P_h) and the net cross sectional free-flow area (A_c) with longitudinal finned tube are given by,

$$P_h = \pi d_{cond,out} + 2H_{fin}N_{fin} \tag{20}$$

$$A_c = H_{cond,box}L_{cond,box} - \left(\pi\frac{d_{cond,out}^2}{4} + N_{fin}\delta_{fin}H_{fin}\right). \tag{21}$$

The empirical correlation proposed by Sieder and Tate (Kakaç, 2002) is used to predict the mean Nusselt number for the water flow in the heat sink,

$$Nu_{HS} = 1.86\left(Pe_{HS}\frac{d_h}{L_{fin}}\right)^{1/3}\left(\frac{\mu_{water}}{\mu_{wall,water}}\right)^{0.14}, \tag{22}$$

where $Pe_{HS} = \mathrm{Re}_{HS}\,\mathrm{Pr}_{HS}$ and the dynamic viscosity in contact with the wall of the finned tube ($\mu_{wall,water}$) is a function of the mean temperature,

$$\bar{T}_{wall,water} = \frac{1}{2}\left(\frac{T_{cond,in} + T_{cond,out}}{2} + \frac{T_{HS,in} + T_{HS,out}}{2}\right). \tag{23}$$

The Reynolds number is determined as,

$$\mathrm{Re}_{HS} = \frac{\rho_{water}v_{HS,water}d_h}{\mu_{water}}, \tag{24}$$

where the equivalent diameter (d_h) based on the pressure drop is defined as,

$$d_h = \frac{4A_c}{P_{wetted}}, \tag{25}$$

where the wetted perimeter (P_{wetted}) of a tube with longitudinal fins is given by,

$$P_{wetted} = 2H_{cond,box} + 2L_{cond,box} + \pi d_{cond,out} + 2H_{fin}N_{fin}. \tag{26}$$

Equation 22 is valid for laminar flow, $0.48 < \mathrm{Pr}_{water} < 16700$ and,

$$\left(Pe_{HS}\frac{d_h}{L_{fin}}\right)^{1/3}\left(\frac{\mu_{water}}{\mu_{wall,water}}\right)^{0.14} \geq 2.$$

The heat transfer coefficient of vapor flow into the condenser tube ($h_{cond,v}$) is estimated from

$$h_{cond,v} = \frac{Nu_{cond,v}\lambda_v}{d_{cond,in}} \tag{27}$$

It is assumed that the flow is fully developed so that the Nusselt number ($Nu_{cond,v}$) can be determined as $Nu_{cond,v} = 4.36$ for laminar regime under constant heat flux and $Nu_{cond,v} = 0.023\mathrm{Re}_v^{0.8}\mathrm{Pr}_v{}^{0.3}$ for turbulent regime.

Where $\mathrm{Re}_v = \dfrac{\rho_v v_{cond,v} d_{cond,in}}{\mu_v}$.

The energy balance in the two-phase region provides:

$$\dot{m}\, h_{lv} = (UA)_{cond,lv}\, \Delta T_{lm}^{cond,lv} \tag{28}$$

where,

$$\Delta T_{lm}^{cond,lv} = \frac{\Delta T_1^{cond,lv} - \Delta T_2^{cond,lv}}{\ln\left(\Delta T_1^{cond,lv} \Big/ \Delta T_2^{cond,lv}\right)}$$

$$\Delta T_1^{cond,lv} = T_{cond,sat} - T_{HS,out}$$

$$\Delta T_2^{cond,lv} = T_{cond,sat} - T_{HS,in}$$

$$(UA)_{cond,lv} = \frac{1}{\dfrac{1}{h_{cond,lv}\left(\pi d_{cond,in} L_{cond,lv}\right)} + \dfrac{\ln\left(d_{cond,out}/d_{cond,in}\right)}{2\pi\lambda_{SS} L_{cond,lv}} + \dfrac{1}{\eta_{fin,0} h_{HS} A_t}}. \tag{29}$$

There are several available correlations to calculate the two-phase heat transfer coefficient ($h_{cond,lv}$). Here the correlation proposed by Cavallini and Zecchin (Kakaç, 2002) is used to determine the two-phase heat transfer coefficient,

$$h_{cond,lv} = 0.05\mathrm{Re}_{eq}^{0.8}\mathrm{Pr}_l{}^{0.33}\frac{\lambda_l}{d_{cond,in}}, \text{ where } \mathrm{Re}_{eq} = \mathrm{Re}_v^{lv}\left(\frac{\mu_v}{\mu_l}\right)\left(\frac{\rho_l}{\rho_v}\right)^{0.5} + \mathrm{Re}_l^{lv}. \tag{30}$$

$Re_l{}^{lv}$ and $Re_v{}^{lv}$ are calculated by

$$\mathrm{Re}_v^{lv} = \frac{\rho_v v_v x d_{cond,in}}{\mu_v}. \tag{31}$$

$$\mathrm{Re}_l^{lv} = \frac{\rho_l v_l\,(1-x)\, d_{cond,in}}{\mu_l} \tag{32}$$

Assuming that there is a linear variation of vapor fraction (x) over a range from 1 to 0 and integrating the Eq. 30 over the two-phase length, $\bar{h}_{cond,lv} = \dfrac{1}{L_{cond,lv}} \displaystyle\int_0^{L_{cond,lv}} h_{cond,lv} dL$, the mean heat transfer coefficient in the two-phase zone can be determined by,

$$\bar{h}_{cond,lv} = 0.028\mathrm{Pr}_l{}^{0.33}\lambda_l\mu_l \left[\frac{\left(\rho_v v_{cond,v} d_{cond,in}\dfrac{\sqrt{\rho_l/\rho_v}}{\mu_l} - \rho_l v_{cond,l}\dfrac{d_{cond,in}}{\mu_l}\right)^{1.8}}{d_{cond,in}^2\left(\rho_v v_{cond,v}\sqrt{\rho_l/\rho_v} - \rho_l v_{cond,l}\right)}\right]. \tag{33}$$

After the determination of the vapor and two phase lengths in the condenser, the liquid length is determined as $L_{cond} = L_{cond,v} + L_{cond,lv} + L_{cond,l}$.

The two-phase pressure drop consists of gravitational pressure drop, frictional pressure drop, and accelerational pressure drop. Since the condenser is placed horizontally, the gravitational pressure drop in the condenser is identically zero. The pressure drop of the two-phase zone in the condenser is estimated using

$$\left(\frac{dp}{dL}\right)_{lv} = \phi_{lv}^2\left(\frac{dp}{dL}\right)_{liq}, \tag{34}$$

where ϕ_{lv} is the two-phase multiplier and $\frac{dp}{dL}$ is the pressure drop in the two-phase ($_{lv}$) and liquid ($_{liq}$) zones.

The single-phase pressure drop for liquid flow in the tube can be written as:

$$\left(\frac{dp}{dL}\right)_{liq} = -\frac{f_{liq}}{d_{cond,in}}\frac{(1-x)^2}{2\rho_{liq}}\left(\frac{\dot{m}}{A_{cond}}\right)^2, \tag{35}$$

where the liquid-phase friction factor (f_{liq}) can be calculated from the Reynolds number as discussed previously for single-phase pressure drop. The Reynolds number of the liquid phase can be calculated as:

$$\mathrm{Re}_{liq} = \frac{4\,\dot{m}\,(1-x)}{\pi\mu_{liq}d_{cond,in}}. \tag{36}$$

Substituting Eq. 35 into Eq. 34 and applying the chain rule, the two-phase pressure drop becomes a function of vapor fraction (x) as,

$$\left(\frac{dp}{dx}\right)_{lv} = -\phi_{lv}^2\frac{f_{liq}}{d_{cond,in}}\frac{(1-x)^2}{2\rho_{liq}}\left(\frac{\dot{m}}{A_{cond}}\right)^2\left(\frac{dL}{dx}\right). \tag{37}$$

Assuming again that there is a linear vapor fraction (x) variation over a 1 to 0 range and integrating the Eq. 37 over the two-phase length, resulting in

$$\Delta P_{lv} = \int_{x=0}^{x=1}\left[-\phi_{lv}^2\frac{f_{liq}}{d_{cond,in}}\frac{(1-x)^2}{2\rho_{liq}}\left(\frac{\dot{m}}{A_{cond}}\right)^2\left(\frac{dL}{dx}\right)\right]dx, \tag{38}$$

where the two-phase multiplier can be determined by,

$$\phi_{lv} = \left(1 + \frac{C}{X} + \frac{1}{X^2}\right)^{0.5} \tag{39}$$

and the Martinelli parameter X can calculated as,

$$X = \left(\frac{f_{liq}}{f_{vap}}\right)^{0.5}\left(\frac{\rho_{vap}}{\rho_{liq}}\right)^{0.5}\left(\frac{1-x}{x}\right). \tag{40}$$

The constant (C) in Eq. 39 is dependent on the flow regime and is associated with the single flow of the vapor and the liquid in the pipe. Table 1 indicates the value of the constant for four different possible combinations.

Table 1. Value of constant (C) in the two-phase correlation proposed by Lockhart and Martinelli.

Liquid	Vapor	C
Turbulent	Turbulent	20
Laminar	Turbulent	12
Laminar	Turbulent	10
Laminar	Laminar	5

4. Results

Several peformance tests were carried out for the LHP and CPL, but only the main results were presented here. Performance tests of one LHP and one CPL, using water as working fluid and a ceramic wick (proposed as an alternative to wicks made of metal and plastic), were carried out for power inputs up to 30 W. The properties of the ceramic porous wick, obtained in (Reimbrecht, 2004), and the working fluids are presented in Table 2.

Figures 5 presents the performance tests of the systems for power inputs up to 15 W and 30 W for the LHP and CPL, respectively. The thermal behavior of the LHP is shown in Fig. 5 (a), drawing attention to the evaporator outlet ($T_{Evap,out}$), condenser inlet ($T_{Cond,in}$), condenser outlet ($T_{Cond,out}$), evaporator inlet ($T_{Evap,in}$), and the compensation chamber (T_{CC}) at horizontal position. The condenser was cooled by a heat sink at temperature of 20 ^{o}C. The LHP has worked satisfactorily in the range from 5 to 15 W. The thermal behavior of the CPL is shown in Fig. 5(b) drawing attention to the the evaporator (T_{Evap}), evaporator outlet ($T_{Evap,out}$), vapor line ($T_{VaporLine}$), condenser inlet ($T_{Cond,in}$), evaporator inlet ($T_{Evap,in}$) and the reservoir (T_{Res}) at horizontal position. The condenser was cooled by air in forced

Table 2. Thermodynamic properties of the ceramic wick and the working fluid.

Wick material	ε (%)	K (m^2)	$\lambda_{eff,sat}$ (W/m-K)	r_p (μ m)
Ceramic[a]	0.50	35×10^{-15}	4.00	$1-3$
Working fluids	σ (N/m)	h_{lv} (kJ/kg)	ρ (kg/m^3)	μ (kg/m-s)
Water[b]	0.07119	2382	995.6	0.0007977

[a] ceramic wick properties were obtianed in (Reimbrecht, 2004).
[b] the properties of the working fluids (at saturation temperature of 40 ^{o} C) were obtianed by the software Engineering Equation Solver (EES).

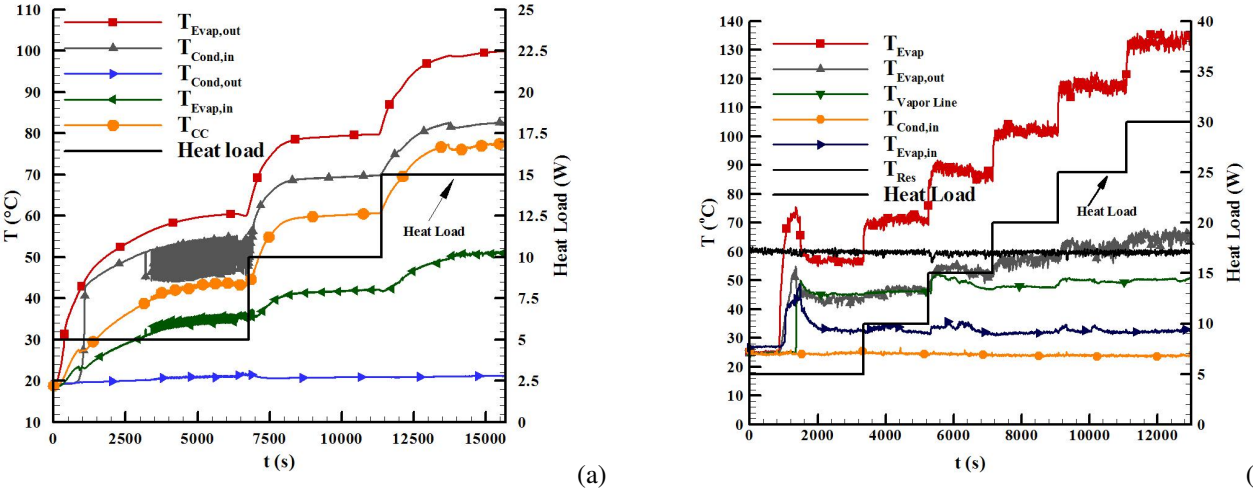

(a) (b)

Figure 5. (a) Temperatures of LHP at heat sink temperature of 20 ^{o}C and (b) CPL for heat loads increasing at horizontal position.

convection. The CPL had a successful startup and reached nearly the steady state for the range of heat load from 5 to 30 W and for reservoir temperature of 60 ^{o}C. It can noticed that there is a difference between temperatures of the evaporator outlet ($T_{Evap,out}$) which is presented in the following.

Figure 6(a) presents the temperatures of the evaporator outlet ($T_{Evap,out}$) of the LHP and the CPL and the evaporator temperature (T_{Evap}) of CPL as a function of the heat load. It can be noticed a large difference between the evaporator outlet temperatures of the LHP and CPL ($T_{Evap,out}$ - CPL) that varied from 19 to 44 ^{o}C. It is clear from Fig. 6(a) that in the results of the CPL, there is a significant difference between the temperature of evaporator (T_{Evap} - CPL) and its outlet temperature ($T_{Evap,out}$ - CPL), varing from 14 to 66 ^{o}C. This difference occurs because the temperature sensor of the evaporator (T_{Evap}) was placed very close to the electric resistor (heating system).

A small temperature difference between the evaporator outlet and the heat sink is required for a successful application of these specific LHP and CPL. Therefore, high temperature differences claim for changes in the properties of the ceramic porous wick (porosity, pore size and thermal conductivity) or improvements in the original design of the systems. A total thermal resistance, similarly to Maydanik et. al. (2009), can be defined as,

$$R_{total} = \frac{(T_{Evap} - T_{HS})}{\dot{Q}_{evap}}, \text{where } T_{HS} \text{ is the heat sink temperature, i.e., the average cooling temperature.} \quad (41)$$

The total thermal was estimated for both systems the LHP and CPL. For the LHP, however, it was considered $T_{Evap,out}$ instead of T_{Evap}, once it was not possible to fix a thermoresistor at the interface between the copper block heater and the evaporator. For the CPL, the heat sink temperature T_{HS} is an average temperature between the inlet and outlet of condenser. Figure 6(b) depicts the total thermal resistance for the LHP and CPL. It is noticed that the total thermal resistance for the CPL even using the evaporator temperature (T_{Evap} - CPL) is lower than LHP. According to the results presented in Fig. 6(b), the total thermal resistance was maximum for heat load of 5 W (5.6 ^{o}C/W for CPL and 10.2 ^{o}C/W for LHP using water) and it was minimum for heat load of 30 W (3.4 ^{o}C/W for the CPL) and heat load of 15 W (5.9 ^{o}C/W for LHP).

The R_{total} is a relative estimation not suitable to take any final conclusions. In this analysis it is not possible any comparison only based on its result. The LHP evaporation area (392.7 mm^2) is half of the CPL one (785.4 mm^2). Additionally, as mentioned before, the heat sink temperatures for both cases are different. Consequently, based only on this result one can not conclude which system worked better. Anyhow, one can say that both systems were successful and

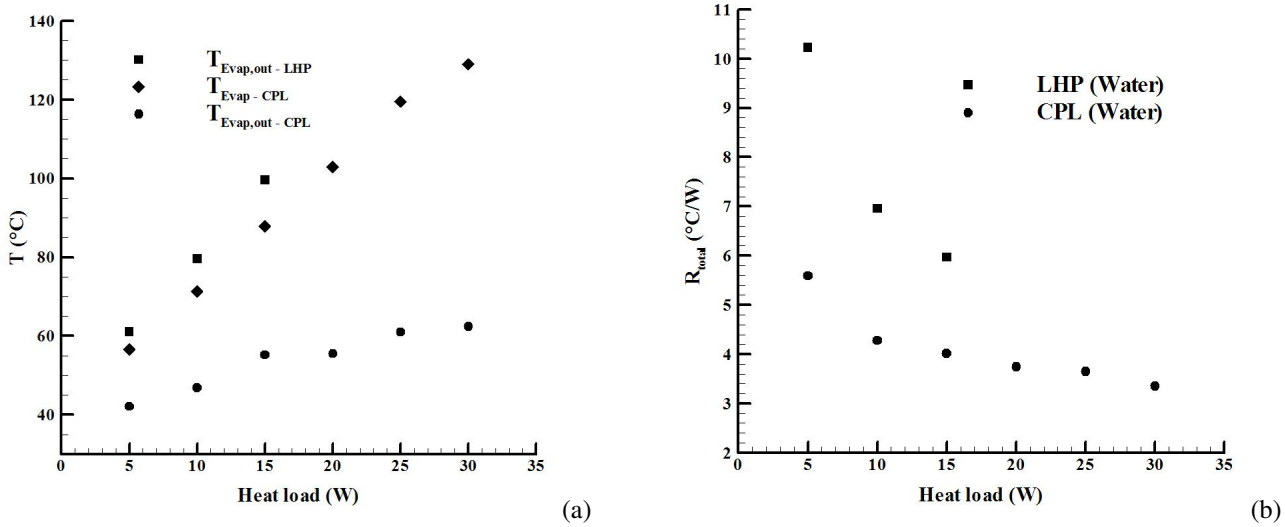

(a) (b)

Figure 6. (a) Outlet evaporator temperature of the LHP and CPL, and evaporator temperature of CPL and (b) total thermal resistance for the LHP and CPL.

could work better for increasing evaporation area (e.g.: increasing the length and/or number of grooves). Even taking into account outlet evaporator temperature ($T_{Evap,out}$) for both systems, it is not possible any direct comparison, once that there is no sufficient control of the assembling, complete vacuum and working fluid filling of the systems. The heat flux were equal to 3.82×10^4 W/m^2 based on the evaporation area for the maximum heat load equal to 15 W for the LHP and 30 for the CPL, respectively.

The pressure drops of the capillary systems were evaluated for the maximum heat load applied to the each system: 15 W for the LHP and 30 W for the CPL. The temperature of the condenser inlet ($T_{Cond,in}$) and the temperature of the reservoir (T_{Res}) were assumed as saturation temperatures of the LHP and CPL, respectively. Table 3 summarizes the estimated results from Section 3 taking into account the dimensions for both the LHP and CPL tested in the lab. For the LHP: $L_{cond,v} = 2$ mm; $L_{cond,lv} = 31$ mm and $L_{cond,l} = 87$ mm. For the CPL: $L_{cond,v} = 48$ mm; $L_{cond,lv} = 40$ mm and $L_{cond,l} = 297$ mm.

Table 3. Pressure drop of the LHP and CPL.

	LHP		CPL	
Components	ΔP (Pa)	%	ΔP (Pa)	%
Vapor grooves	99.13	15.83	1088.00	42.41
Vapor transport line	44.51	7.11	173.40	6.76
Porous wick	480.00	76.65	1291.00	50.32
Liquid transport line	0.52	0.08	1.75	0.07
Two phase zone of condenser	2.08	0.33	11.26	0.44
Total pressure drop	**626.24**	**100.00**	**2565.00**	**100.00**
Capillary limit	**41780.00**	-	**44157.00**	-

Note that the total pressure drop of the both systems do not overcome the capillary limit and the total pressure drop of the LHP is smaller than the CPL one. It can be also noticed that porcentage of pressure drop in the vapor and liquid transport lines and in the two phase zone of condenser are almost the same. However, the porcentage of the pressure drop in the grooves and in the porous wick are different. So, the fact of the total pressure drop of the CPL is greater than the LHP one is due to, according to the Eqs. 6 and 8 (which depend on the number of the grooves), the greater number of grooves in the evaporator of the CPL.

According to Ku (1994) and Ku (1999) and others researchers, the pressure drop across the two phase zone into the condenser can be neglected when compared with the total pressure drops of the capillary pumping systems. As it can be noticed in Table 3, the two phase pressure drop into the condenser is very small representing less than 0.5%, due to low mass flow rates and its calculation can be neglected.

5. Conclusions

The ceramic wick here proposed as alternative to wicks made of metal and plastic showed a reliable alternative for applications in LHPs and CPLs. Performance tests of one LHP and one CPL with a ceramic wick and using water as working fluid were carried out for power inputs up to 30 W. For higher power inputs, temperatures above $100\ ^oC$ were measured. The LHP worked satisfactorily in the range from 5 to 15 W and the CPL worked satisfactorily from 5 to 30 W. The corresponding minima total thermal resistances were $3.4\ ^oC/W$ for the CPL and $5.9\ ^oC/W$ for LHP.

Both systems could work better for increasing evaporation area (e.g.: increasing the length and/or number of grooves). The heat fluxes for the maximum heat load (15 W for LHP and 30 W for CPL) for both systems were equal to 3.82×10^4 W/m^2.

The systems did not overcome the capillary limit for their maxima heat loads, making possible significant increase of the vapor and liquid transport lines. Further studies are planned considering similar geometry and operation conditions with new experiments.

6. References

Berti, L.F., 2008, "Characterization of Porous Wicks for Application in Capillary Pumping Systems", Dissertation (in portuguese), Federal University of Santa Catarina, Brazil.

Holman, J.P., 1990, "Heat Transfer", McGraw-Hill, 7th Edition.

Kakac, S. and Liu, H., 2002, "Heat Exchangers Selection, Rating, and Thermal Design", CRC, 2nd Editon.

Ku, J., 1994, "Thermodynamic Aspects of Capillary Pumped Loop Operation", Proceedings of the 6th AIAA/ASME Joint Thermophysics and Heat Transfer Conference, AIAA-94-2059, Colorado Springs, USA, pp.1-11.

Ku, J., 1999, "Operating Characteristics of Loop Heat Pipes", Proceedings of the 29th International Conference on Enviromental System, Denver, Colorado, USA.

Maydanik, Y. F. and Vershinin, S., 2009, "Development and tests of ammonia miniature loop heat pipes with cylindrical evaporators", Applied Thermal Engineering, vol. 29, pp. 2297-2301.

Rassamakin, B. M., Pismenny, Y. N., Khayrnasov, S. M., Ye, Y. and Smirnov, G. F., 2002, "Research and Development of Aluminum Loop Heat Pipes Operation Characteristics", Proceedings of the 12 th IHPC, Moscow.

Reimbrecht, E.G., 2004, "Manufacturing, Geometric Characterization and Determination of Hydraulic Properties of Porous Wicks for Using in Capillary Pumps", Thesis (in portuguese), Federal University of Santa Catarina, Brazil.

Rhi, S. H., 2006, "Operation and Characteristics of a Loop Heat Pipe", Proceedings of the 8th International Heat Pipe Symposium, Kumamoto, Japan.

Santos, P.H.D., Bazzo, E., Becker, S., Kulenovic, R. and Mertz, R., 2010, "Development of LHPs with Ceramic Wick", Applied Thermal Engineering, Vol. 30, pp. 1784-1789.

7. Responsibility Notice

The authors are the only responsible for the printed material included in this paper